Journal of Medicinal Chemistry

Article

Discovery of an Orally Active Small Molecule TNF-# Inhibitor

Weiguang Sun, Yanli Wu, Mengzhu Zheng, Yueying Yang, Yang Liu, Canrong Wu, Yirong Zhou, Yonghui Zhang, Lixia Chen, and Hua Li

J. Med. Chem., **Just Accepted Manuscript** • DOI: 10.1021/acs.jmedchem.0c00377 • Publication Date (Web): 15 Jul 2020

is published by the American Chemical Society. 1155 Sixteenth Street N.W., Washington, DC 20036

Discovery of an Orally Active Small Molecule TNF-α Inhibitor

Weiguang Sun[†, #], Yanli Wu[‡, #], Mengzhu Zheng[†, #], Yueying Yang[‡], Yang Liu[‡], Canrong Wu[†], Yirong Zhou[†, *], Yonghui Zhang[†, *], Lixia Chen[‡, *], Hua Li[†, ‡,*]

† Hubei Key Laboratory of Natural Medicinal Chemistry and Resource Evaluation, School of Pharmacy, Tongji Medical College, Huazhong University of Science and Technology, Wuhan 430030, China

‡ Wuya College of Innovation, Key Laboratory of Structure-Based Drug Design & Discovery, Ministry of Education, Shenyang Pharmaceutical University, Shenyang 110016, China

ABSTRACT: Tumor necrosis factor α (TNF-α) is an important therapeutic target for rheumatoid arthritis, inflammatory bowel disease and septic hepatitis. In this study, structure-based virtual ligand screening combined with *in vitro* and *in vivo* assays was applied. A lead compound, benpyrine, could directly bind to TNF-α and block TNF-α-trigged signaling activation. Furthermore, endotoxemia murine model showed that benpyrine could attenuate TNF-α-induced inflammation, thereby reducing liver and lung injury. Meanwhile, administration of benpyrine by gavage significantly relieved the symptoms of collagen-induced arthritis and imiquimod-induced psoriasiform inflammation in mice. Thus, our study discovered a novel, highly specific and orally active small molecule TNF-α inhibitor that is potentially useful for treating TNF-α mediated inflammatory and autoimmune disease.

■ INTRODUCTION

Tumor necrosis factor α (TNF-α), which is mainly secreted by active macrophages and monocytes, is a pleiotropic cytokine that plays crucial roles in immune functions, including inflammation, antitumor responses, and infections.[1] An elevated serum level of TNF-α is associated with tumorigenesis, diabetes, and particularly autoimmune disorders, such as rheumatoid arthritis (RA), psoriatic arthritis, multiple sclerosis, and Crohn's disease.[2] Therefore, direct inhibition of TNF-α has become a major therapeutic approach for the treatment of these diseases. The well-known commercial monoclonal antibodies adalimumab and infliximab, and the fusion protein etanercept have been proven to directly bind to TNF-α, further preventing its interaction with the tumor necrosis factor receptor (TNFR).[3, 4] To date, these biomacromolecular agents have shown excellent therapeutic effects and high specificity for the treatment of autoimmune diseases.[5] However, several severe limitations, such as poor stability, cost-ineffective commercial-scale production, and serious side effects, have also emerged, prompting the demand for novel small molecule TNF-α inhibitors.[6]

To date, several selective small molecule antagonists of TNF-α have been identified, most of which engender the inhibitory effects by targeting key molecules of the intracellular TNF-α pathway, inhibiting TNF-α converting enzyme (TACE) or down-regulating the expression of TNF-α.[7] Although progress has been made in developing small molecules that are capable of directly disrupting TNF-α and TNFR interactions, this area of research remains a huge challenge. To our knowledge, some small molecules that directly antagonize TNF-α, such as the polysulfonated

naphthylurea suramin analogues and the indole-linked chromone derivative SPD304, often show low potency, poor selectivity, and tend to cause adverse side effects, making them unsuitable for anti-TNF-α therapies.[8-10] Furthermore, SPD304, which contains a toxic 3-alkylindole moiety, is metabolized by cytochrome P450 enzymes through a dehydrogenation pathway similar to that of the potent pneumotoxin 3-methylindole, producing reactive electrophilic iminium materials that could react with protein and DNA targets.[11]

Thus, additional efforts to identify effective and highly specific TNF-α inhibitors with relatively lower toxicity are urgently demanded.[12-14] In the present study, a novel small molecule inhibitor targeting TNF-α was identified using a structure-based virtual screening method in combination with *in vitro* and *in vivo* activity assays.

■ RESULTS AND DISCUSSION

Structure-based virtual ligand screen for TNF-α inhibitors. In this study, the X-ray co-crystal structure of a TNF-α dimer with SPD304 (PDB code: 2AZ5) was used as the model to screen 6 million drug-like compounds from the ZINC database *in silico*. The top seven highest scoring compounds (**1-7**) were selected from the initial high-throughput virtual screening campaign. Subsequently, we applied these compounds at concentrations of 1 and 10 μM in the initial tests to examine their ability to inhibit TNF-α-induced cytotoxicity in L929 cell line. Compound **7**, (S)-4-((9H-purin-6-yl)amino)-1-benzylpyrrolidin-2-one, which was designated benpyrine, exhibited dose-dependent inhibitory effects that were consistent with the

screening result. Therefore, this compound was selected for further characterization and functional validation *in vitro* and *in vivo*.

Benpyrine directly binds to TNF-α. The microscale thermophoresis (MST) method was utilized to assess the ability of these compounds binding to TNF-α and to further validate the results of the molecular docking simulations.[15, 16] Encouragingly, the K_D value of benpyrine (82.1 ± 5.0 μM) was even smaller than that of SPD304 (91.7 ± 6.3 μM). In comparison, no statistically significant binding was detected when TNF-α was treated with compounds **1-6** (Table S1 and Figure S1 in SI). Based on these data, benpyrine and SPD304 displayed relatively stronger binding affinity to TNF-α. Another MST assay was performed to further determine whether the direct binding between benpyrine and TNF-α was related to the interaction between TNF-α and TNFR1 or not. Briefly, after incubation with 10 μM benpyrine for 30 min, the K_D value of TNF-α-TNFR1 binding was increased approximately 18-fold (from 0.23 μM to 4.26 μM) comparing with the interaction in the absence of benpyrine. In addition, the K_D value was further increased to 19.63 μM after the addition of 100 μM benpyrine (Figure 2A-2D). All these results confirmed the specific binding of benpyrine to TNF-α, and partially confirmed that benpyrine suppressed the binding of TNF-α to TNFR1. Meanwhile, the ELISA assay further revealed that benpyrine tightly bound to TNF-α and blocked its interaction with TNFR1, with an IC_{50} value of 0.109 μM (Figure 2E). A drug affinity responsive target stability (DARTS) assay and protein thermal shift (PTS) assay were performed using published methods to further validate the targeting of TNF-α by benpyrine.[17, 18] As shown in Figure 2F, most of the

TNF-α was degraded within 30 min after the pronase treatment, whereas the degradation of TNF-α in benpyrine-treated samples was decreased in a dose-dependent manner. And in Figure 2G, benpyrine increased the thermal stability of TNF-α protein from tolerated temperature of 90 °C to 94 °C. Thus, benpyrine inhibits TNF-α activity by directly binding to the protein.

Analysis of the binding mode. The binding pocket of the TNF-α dimer is relatively large and featureless, lacking clearly defined binding crevices.[19] The binding site is mostly hydrophobic, consisting primarily of glycine, leucine, isoleucine and tyrosine residues. Based on the generated docking model, as expected, the binding of benpyrine to TNF-α was a relatively hydrophobic interaction driven by the shape to prevent the binding of the third subunit, which forms the biologically active trimer complex. As shown in Figure 2H and 2I, benpyrine adopted a clamp-shaped conformation and formed several hydrophobic interactions with Leu57, Tyr59, Tyr119, Gly121 and Tyr151 from both TNF-α monomers. No predicted hydrogen bonding interactions were observed.

According to the predicted binding sites for benpyrine in TNF-α, several site-directed mutations, including $L^{57}A$, $Y^{59}A$, and $Y^{119}A$, were introduced. The MST assay revealed a weaker binding affinity of benpyrine for the $L^{57}A$ and $Y^{59}A$ mutants than wild type TNF-α, while no obvious changes in the binding affinity for the $Y^{119}A$ mutant were observed. The efficacy and specificity of benpyrine-mediated inhibition of TNF-α mutant-induced L929 cells death was further determined. As shown in Figure 3A-3C, all TNF-α mutants significantly induced L929 cell death, with IC_{50}

values ranging from 3.21 to 6.36 ng/mL in combination with 1 μg/mL actinomycin D. However, benpyrine only blocked cell death induced by TNF-α^{WT} and $Y^{119}A$ and, increased the cell survival rate up to 80%. Meanwhile, benpyrine did not obviously affect $L^{57}A$- and $Y^{59}L$-induced cytotoxicity in L929 cells. Thus, Leu^{57} and Phe^{59} are the key amino acids required for the binding of benpyrine, consistent with the docking prediction.

Benpyrine blocks TNF-α-induced signaling pathways. TNF-α-induced inflammatory process is under the control of several sequences in gene promoters.[20] In particular, the stimulation of the nuclear factor kappa-B (NF-κB) transcription factor has attracted increasing attentions. NF-κB has recently been shown to induce the expression of a variety of antiapoptotic factors, which are important for regulating the TNFR1-mediated activation of apoptotic mechanisms.[21] In the present study, we investigated the effects of benpyrine on the activation of the NF-κB pathway in RAW264.7 macrophages. After an incubation with different concentrations of benpyrine for 12 h, TNF-α (10 ng/mL) or lipopolysaccharide (LPS, 1 μg/mL) was added and incubated for another 2 h. Protein lysates were subjected to western blotting with anti-IκBα and p-IκBα antibodies. In the absence of benpyrine, TNF-α and LPS induced the phosphorylation of inhibitor of NF-κB α (IκBα). Encouragingly, a pretreatment with benpyrine resulted in a dose-dependent decrease in the phosphorylation of IκBα (Figure 3D and 3E). These observations were also consistent with the result of the microscopy analysis shown in Figure 3F. In this experiment, the addition of benpyrine abolished the TNF-α-induced nuclear translocation of

NF-κB/p65 in RAW264.7 cells. Furthermore, benpyrine exhibited low cytotoxicity toward RAW264.7 cells (IC_{50} > 100 μM), indicating that benpyrine represents a potentially hypotoxic TNF-α inhibitor.

Benpyrine inhibits the LPS-induced production of inflammatory cytokines *in vivo.* LPS causes a systemic inflammatory response and acute tissue injury when injected into mice as an endotoxin.[22] Here, the effect of benpyrine on LPS-triggered inflammatory responses was examined *in vivo*. Mice were preinjected with the vehicle or benpyrine, followed by the administration of normal saline (NS) or LPS (1.5 mg/kg). As shown in Figure 4, serum levels of inflammatory cytokines, including IL-6 and IL-1β, were substantially increased in mice treated with LPS compared with the control group, while the increased levels of these cytokines was substantially attenuated by pretreating mice with different concentrations of benpyrine.

The anti-TNF-α effects of benpyrine on an animal model of megadose endotoxemia were further studied. The benpyrine pretreatment (25 mg/kg) significantly increased the survival rate compared with the non-treated control group. According to the histopathology, the benpyrine treatment significantly reduced the liver and lung damage and emergence of hemorrhagic necrosis caused by the LPS treatment. Based on these results, benpyrine has great potential to serve as an anti-inflammatory agent.

Therapeutic effects of benpyrine on mice with type II collagen-induced arthritis (CIA). Rheumatoid arthritis (RA) is the most common chronic inflammatory autoimmune disorder affecting the synovial joints, with approximately 1% of the global population suffering from this disorder.[23, 24] Inflammatory cytokines such as TNF-α, interleukin (IL)-6, IL-1 and IL-17 play important roles in RA pathogenesis, while an anti-TNF-α treatment effectively slows disease progression among the various anti-rheumatic methods.[25, 26] CIA is an autoimmune model manifesting common immunological and pathological features associated with human RA, including synovial hyperplasia, cartilage destruction, and immune hyperfunction. In the present study, the benpyrine treatment significantly decreased the arthritic score and spleen index of CIA mice compared with the untreated group (Figure 5A and 5B). The regulation of inflammatory mediators was speculated to be important in the pathogenesis and therapy of RA. Therefore, serum levels of IFN-γ, IL-1β IL-6, and IL-10 were measured using ELISA analysis. As shown in Figure 5C-F, serum levels of these cytokines were much higher in the non-treated CIA mice, suggesting the induction of an obvious inflammatory response in the model group. Benpyrine dose-dependently decreased the levels of proinflammatory cytokines, such as IFN-γ, IL-1β and IL-6, and increased the concentration of the anti-inflammatory cytokine IL-10.

The effects of benpyrine on the joints of rats were determined by performing histochemical staining with H&E. As shown in Figure 5G, a normal joint histology was observed in the control group. The ankle and toe joints of mice in the CIA group

showed significant histopathological changes related to severe arthritis, including notable synovial hyperplasia, partial bone and cartilage destruction, inflammatory cell infiltration into the synovium, and narrowing of the joint space. In contrast, benpyrine and prednisone (Pro, 5 mg/kg) significantly ameliorated the degree of cartilage and bone destruction and inflammation compared with the CIA group.

Therapeutic effects of benpyrine on imiquimod-induced psoriasiform inflammation in mice. Psoriasis is a chronic inflammatory skin disease affecting 2–3% of the global population.[27, 28] Despite the extensive studies, the detailed mechanism underlying the pathogenesis of psoriasis remains to be elucidated. Initially, psoriasis was described as a disease involving the excessive proliferation of keratinocytes that subsequently triggered inflammation. Several neutralizing anti-TNF agents, such as etanercept and infliximab, have been successfully applied to treat psoriasis.[29, 30] Indeed, the amelioration achieved with TNF antagonists confirms that TNF-α is a pivotal proinflammatory mediator in psoriatic lesions.

The mouse model of imiquimod-induced psoriasiform inflammation (IPI) was employed to evaluate the effects of benpyrine on psoriasis. Compared to the psoriatic mouse models using a skin xenograft, gene knockout, or gene mutation, this model represents a better tool for the investigation of the pathogenesis and therapeutic agents of psoriasis because it can be elicited in a more natural immune state.[31] The mice in the model group displayed erythema, scales, and incrassation on their back skin beginning on day 2, and these symptoms were most visible on day 5. After treatment with benpyrine, differences in the skin were observed between all groups. Compared

to the IPI model mice, the benpyrine treatment inhibited inflammation throughout the period of imiquimod exposure and significantly decreased the adjusted scale scores consisting of erythema, epidermal acanthosis, and the thickness of the lesions (Figure 6A-B). The benpyrine treatment also reduced the spleen index, which was distinctly increased after the imiquimod application (Figure 6C). Proinflammatory cytokines, such as IL-1β, IL-17F, IL-22, IL-6, *etc*., are crucially involved in psoriatic skin inflammation. The serum levels of the proinflammatory cytokines IL-1β and IL-6 were further examined to obtain additional insights into the therapeutic effects of benpyrine. As revealed by the ELISAs, the levels of IL-1β and IL-6 were significantly increased in the IPI mice, while benpyrine dose-dependently decreased this increase in the IL-1β and IL-6 levels after 7 days of treatment. Its efficacy was comparable to prednisone at 5 mg/kg (Figure 6D-E). Additionally, histopathological changes induced by the benpyrine group were obviously ameliorated compared to IPI mice (Figure 6F).

■ CONCLUSIONS

TNF-α is mainly secreted by active monocytes or macrophages and is a well-known pleiotropic cytokine with crucial roles in the host immune system. Over-expression of TNF-α is a hallmark of many inflammatory diseases, including rheumatoid arthritis, psoriasis, inflammatory bowel disease and septic shock, making it an excellent therapeutic target for clinical interventions.[32-34] Significant advances have been made in the development of biological agents targeting TNF-α and its signaling components. Several well-known commercial TNF-α inhibitors, such as infliximab, adalimumab

and etanercept, are TNF-α antibodies or TNFR1-Fc chimeras.[35, 36] The anti-TNF-α drugs specifically bind to the TNF-α protein, thus preventing it from binding to the receptors, TNFR1 and TNFR2.[37] To date, those biomacromolecular agents have been proven to be effective treatments for inflammatory bowel disease and rheumatoid arthritis due to their high specificity. According to an industry analysis, TNF-α antibodies account for over 30 billion dollars of the global antibody market. However, several severe limitations, including poor stability, cost-ineffective commercial-scale production, and exclusion by the blood/brain barrier, have also emerged. Instead, small molecule compounds have been appreciated as appropriate alternatives for overcoming most disadvantages associated with macromolecular inhibitors. Furthermore, they offer additional clinical benefits, such as a simpler preparation for oral medicine.[38, 39]

To date, several selective small molecule antagonists of TNF-α activity have been identified. However, none of these small molecule inhibitors have been reported to reduce TNFα-induced inflammatory responses *in vivo* with high efficiency and low toxicity. In this study, we applied the virtual screening technique to discover small molecule antagonists of TNF-α, enabling us to identify the lead compound benpyrine that potently inhibits TNF-α-induced cytotoxicity.

The formation of a trimer of TNF-α is a requirement for its binding to two receptors, TNFR1 (also called CD120a) and TNFR2 (also called CD120b). The engagement of TNF-α with TNFR1 and TNFR2 initiates signaling cascades that result in inflammatory responses and control apoptosis. In this study, we took advantage of

the crystal structure of the TNFα/SPD304 complex and utilized it as the basis for the virtual ligand screening. The molecular docking simulations suggested that benpyrine formed the key hydrophobic interactions with Leu57 and Phe59, which blocked the formation of the TNF-α trimer. This prediction was further confirmed by studying mutant proteins. The $L^{57}A$ and $Y^{59}L$ mutations markedly attenuated the protective effects of benpyrine on the death of L929 cells induced by these mutants. Additionally, benpyrine displayed the decreased binding affinities for these mutants in the MST assay. Meanwhile, benpyrine significantly inhibited TNF-α- and LPS-induced phosphorylation of IκBα and abolished the TNF-α induced nuclear translocation of p65 in RAW264.7 cells. Taken together, these results establish the function of benpyrine as a potent TNF-α inhibitor.

In addition to its efficacy *in vitro*, benpyrine significantly attenuated TNF-α-induced inflammation *in vivo*, and thus shows promise as a potential therapeutic agent for TNF-α-mediated inflammatory diseases. In the mouse model of LPS-induced endotoxemia, benpyrine remarkably decreased the death rate of mice. Furthermore, benpyrine also exerted therapeutic effects on collagen-induced arthritis and imiquimod-induced psoriasiform inflammation in mouse models. Benpyrine showed superior therapeutic effects and obviously decreased the scale scores of illnesses consisting of inflammatory and hyperactive immune reactions. Moreover, the acute toxicity test confirmed the lack of toxicity of benpyrine at the dose of 2000 mg/kg (by gavage), thus validating its safety. Benpyrine is an effective small

molecule inhibitor of TNF-α that could be potentially useful as a therapeutic intervention for various inflammatory diseases.

■ EXPERIMENTAL SECTION

Reagents. The compound collection, including compounds **1-7**, was obtained from AnalytiCon Discovery (Molport, Latvia). The ZINC database (http://zinc.docking.org/) is publicly available and can be accessed free of charge. SPD304, LPS, and prednisone were purchased from Sigma-Aldrich (St. Louis, MO, USA). The TNF-α cDNA was synthesized by GENEWIZ (Suzhou, China). TNFR-1 was obtained from Prospec (Rehovot, Israel). Mouse monoclonal antibodies against IκBα, p-IκBα, and NF-κB/p65 were provided by Cell Signaling Technology (Boston, MA, USA). The L929 and RAW264.7 cell lines were purchased from Boster Bioengineering Company (Wuhan, China). For the further animal experimrnts, more compound **7** was total systhesis as described in Scheme S1 of SI. Purity of compound **7** was determined to be higher than 95% by HPLC analysis which was performed on Daicel CHIRALCEL IC column (250 mm × 10 mm, 5 μm) and method as: MeCN : H_2O = 30 : 70 by 20 min of isocratic hold, a flow rate of 2.0 mL/min, and plotted at 254 nm;

Animals. Balb/c mice (18–20 g) were purchased from the Laboratory Animal Center of Tongji Medical College of Huazhong University of Science and Technology (Wuhan, China). All animals were acclimated for 7 days before being used in the experiment. Mice were housed under pathogen-free conditions at

temperature of 22 ± 2 °C, humidity of 55 ± 5%, and a 12-h light/dark cycle. They had free access to water and food under standard specific pathogen-free (SPF) conditions throughout the study. All animal experiments were carried out in accordance with protocols approved by the Institutional Animal Care and Use Committee at the Tongji Medical College of Huazhong University of Science and Technology (NO. 2019-S972).

Virtual screening and molecular docking simulations. Lead-like compound libraries from the ZINC database containing over 600,000 compounds were screened *in silico*. Molecular docking was performed using the ICM-Pro 3.8.2 program (MolSoftLLC, San Diego, CA).[40] According to the internal coordinate mechanics (ICM) method, the molecular system is based on the internal coordinates (IC) representation of molecular objects that naturally reflects the covalent bond geometry of molecules. For structure predictions and large-scale conformational sampling, ICM employs a family of new global energy optimization techniques, including biased probability Monte Carlo simulations, a pseudo-Brownian docking algorithm[3] and local deformation loop movements.

The initial model of TNF-α was built from the X-ray co-crystal structure of the TNF-α dimer with SPD304 (PDB code: 2AZ5) using a previously reported procedure. Hydrogens and missing heavy atoms were added to the receptor structure, followed by local minimization by using the conjugate gradient algorithm and analytical derivatives in the internal coordinates. In the docking analysis, the binding site was assigned across the entire structure of the protein dimer. ICM docking was performed

to identify the most favorable orientation. The resulting trajectories of the complex between the small molecules and TNF-α dimer were energy minimized, and the interaction energies, which are expressed in kJ/mol, were computed. As a reference, the molecular docking of the well-known TNF-α inhibitor SPD304 showed a score of -32.9.

Expression and purification of recombinant wild type and mutant TNF-α. The gene encoding TNF-α was cloned into the pET-28a vector (Novagen). After verifying the sequence, the recombinant plasmid was transformed into *E. coli* BL21 (DE3) (Invitrogen) cells that were grown in LB medium at 37 °C to an OD600 (0.8-1.0), and expression was induced with 0.4 mM isopropyl-D-thiogalactopyranoside (IPTG) at 20 °C for 16 h. Bacterial cells were collected and lysed by ultrasonication on ice in a buffer containing 20 mM Tris, pH 8.5, 200 mM NaCl, 5 mM mercaptoethanol, 0.1% TritonX-100, and 5% glycerol. Soluble C-terminally hexa-histidine-tagged TNF-α was bound to Ni-agarose affinity resin (Qiagen), washed with a buffer containing 20 mM Tris, pH 8.5, 200 mM NaCl, and 10 mM imidazole, and eluted with a buffer containing 20 mM Tris, pH 8.5, 250 mM NaCl, and 150 mM imidazole. Thrombin (Roche) was added to the eluate at a concentration of one unit per 4 mg of protein, which was then dialyzed against 20 mM Tris, pH 8.5, and 100 mM NaCl at room temperature for overnight digestion. The protein was further purified with anion exchange chromatography using a linear gradient of 10 mM to 1 M NaCl and size exclusion chromatography in 20 mM Tris, pH 8.5, and 200 mM NaCl.

Analysis of the direct binding of compounds 1-7 to TNF-α with MST. TNF-α was labeled with the Monolith NT™ Protein Labeling Kit RED (Cat#L001) according to manufacturer's labeling protocol. Labeled TNF-α was maintained at a constant concentration of 100 nM, while all tested samples were diluted in 20 mM HEPES (pH 7.5) containing 0.05% (v/v) Tween-20. Compounds were sequentially diluted covering the range of appropriate concentrations. After a 10 min incubation at room temperature, samples were loaded into Monolith™ standard-treated capillaries and the thermophoresis was measured at 22 °C using 100% light-emitting diode (LED) and 20% MST power on a Monolith NT.115 instrument (NanoTemper Technologies, München, Germany). The values of the dissociation constant K_D were fitted using the Nanotemper Analysis software v.1.2.101. The TNFR1 protein was also labeled as described above, and the binding of TNFR1 to TNF-α or benpyrine was also tested. Furthermore, after 10 or 100 μM benpyrine was preincubated with various concentrations of TNF-α at room temperature for 15 min, the mixture was added to an equivalent volume of labeled TNFR1 to determine the K_D value.

Determination of the inhibitory effect of benpyrine on the interaction between TNFR1 and TNF-α using an ELISA. Microtiter plates were coated with TNFR1 (2.5 μg/mL) in PBS overnight at 4 °C. The wells were washed three times with PBS/0.05% Tween 20 (PBST), blocked with 200 μL of PBST containing 1% BSA for 60 min and washed as described above. Serial dilutions of benpyrine in 50 μL of PBS containing 2% DMSO were added to the wells, and the microtiter plates were incubated with shaking for 20 min. TNF-α (0.01-10 μg/mL) in 50 μL of PBS

was added to the wells and the plates were incubated for an additional 120 min. The plates were washed as described above and incubated with the TNF-α antibody (1:1000) in 100 μL of PBST containing 1% BSA for 120 min. The plates were washed five times with PBST and incubated with a horseradish peroxide-conjugated secondary antibody for 120 min. The plates were washed as described above, incubated with 100 μL of the TMB solution, quenched with 100 μL of 2 N sulfuric acid, and the absorbance was measured at λ = 450 nm.

Evaluation of the cellular susceptibility to TNF-α proteins and neutralizing bioactivity of benpyrine. Cytotoxicity toward L929 cells was analyzed using previously described methods, with some modifications. A confluent monolayer of L929 cells was trypsinized and resuspended in RPMI-1640 at a density of 1×10^5 cells/mL. One hundred microliters of suspended cells (2×10^5 cells/mL) were seeded in each well of a 96-well tissue culture plate. The medium was discarded after an overnight culture and replaced with RPMI-1640 containing various concentrations of recombinant human TNF-α and 1 μg/mL actinomycin D. The CCK8 assay was conducted after 24 h of culture at 37 °C. The sensitivity of L929 cells to TNF-α was analyzed using a similar procedure without actinomycin D exposure.

In this experiment, 2.0 ng/mL TNF-α was incubated with various concentrations of benpyrine for 2 h at 37 °C in a 96-well plate prior to the addition of 5×10^4 L929 cells/mL to measure the ability of the selected compounds to neutralize the bioactivity of human TNF-α in L929 cells. The assay mixture in a total volume of 100 μL was incubated at 37 °C for 24 h. The inhibition rate of L929 proliferation was measured

with a colorimetric assay using the CCK8 method. IC_{50} values were calculated according to the Reed-Muench method.

Evaluation of the inhibitory effect of benpyrine on TNF-α-stimulated activation of the NF-κB pathway. RAW264.7 cells (5×10^4 cells/mL) were cultured overnight. Then, 5, 10 or 20 μM benpyrine was added and incubated for 12 h; 10 ng/mL TNF-α or 1 μg/mL LPS was added and incubated for another 2 h. Then, the cellular proteins were extracted with RIPA lysis buffer (Beyotime, China). The protein concentration was measured using the BCA assay (Beyotime, China). Equal amounts of protein samples were separated by 12% sodium dodecyl sulfate polyacrylamide gel electrophoresis and then transferred onto PVDF membranes. After blocking with 5% non-fat milk for 2 h at room temperature, the PVDF membranes were incubated with the primary antibodies at 4 °C overnight and subsequently with HRP-conjugated secondary antibodies at room temperature for 2 h. The protein bands were detected using ECL reagents. Chemiluminescent signals were detected and analyzed using the ChemiDoc XRS imaging system (Bio-Rad, USA).

RAW 264.7 cells were grown to 50–70% confluence in a glass chamber, pretreated with DMSO or benpyrine for 12 h, and then stimulated with 10 ng/mL TNF-α for 2 h. Cell treatments were terminated by washing the cells with PBS, followed by fixation with freshly prepared 4% paraformaldehyde in PBS for 20 min. The fixed cells were washed three times with PBS and then permeabilized with 0.25% Triton X-100 in PBS for 10 min. After blocking with 2 mg/mL BSA for 1 h at room temperature, we added the NF-κB/p65 antibody at a 1:1000 dilution at 4 °C overnight,

washed three times with PBS, then incubated with a 1:500 dilution of the secondary antibody for 1 h at room temperature in dark. Finally, DAPI was used to stain the nuclei at 37 °C for 30 min in dark. Images of the cells were captured and analyzed using a Nikon eclipse microscope.

Acute toxicity test. Acute toxicity was tested using a variation of the method described in a previous study.[41] After a 12 h fast, Balb/c mice (18-22 g) were treated with a dose of benpyrine (2000 mg/kg) by gavage. Animals administered 1% CMC-Na served as controls. The animals were observed continuously for 1 h to monitor any gross behavioral changes and death, intermittently for the next 6 h, and then again one week after dosing with benpyrine.

Analysis of LPS-induced changes in the levels of proinflammatory cytokines. Cytokines were assessed by measuring serum concentrations. Male Balb/c mice aged 7–8 weeks were randomly assigned into four groups: the control, LPS and benpyrine (25 or 50 mg/kg) groups. Mice treated with the compound were orally administered benpyrine for 90 min, and then the mice (LPS group, benpyrine-treated group) were intraperitoneally injected with LPS (1.5 mg/kg). Mice in those groups were euthanized and their serum was separated from clotted blood at 4 h after the administration of LPS. Serum was stored at -80 °C, and concentrations of the cytokines IL-1β and IL-6 were measured with a sandwich ELISA using commercially available reagents according to the manufacturer's instructions (Wuhan Boster Bio-Technology). Serum samples were obtained from at least six mice in each group and analyzed in duplicate.

Thirty mice were randomly divided into the following 3 groups (n=10 mice per group) to further evaluate the effect of benpyrine on the survival of mice with LPS-induced endotoxemia (15 mg/kg, i.p.): control (NS, i.p.), LPS (15 mg/kg, i.p.), LPS + benpyrine (25 mg/kg, i.g.). Benpyrine (i.g.) was administrated 2 h before the LPS injection. Saline or benpyrine was administrated 2 h before the injection of LPS and at 12, 24, 48, 72 and 96 h after the injection of LPS. Survival was monitored daily for up to 2 weeks. Liver and lung tissues were collected and fixed with 10% formalin, and sections were stained with hematoxylin and eosin.

Induction of CIA and drug administration. Briefly, the normal group consisting of 10 mice was randomly assigned before the experiment and did not undergo immunization, while the model and treatment groups were immunized as described below. Bovine type II collagen (Chondrex, USA) was dissolved in 0.1 M acetic acid at a concentration of 2 mg/mL and stored at 4 °C overnight, and then it was emulsified with an equal volume of Freund's complete adjuvant (CFA) (Sigma, USA) to a final concentration of 1 mg/mL. On the 1st day of the experiment, all mice were intradermally injected with the CII emulsion at several sites at the base of the tail, with a total volume of 0.1 mL per mouse, as the primary immunization. Two weeks after the primary immunization (on the 14th day), the mice were challenged again by injecting the same volume of the CII emulsion at the same location. The mice in the benpyrine groups (i.g. 25, 50 mg/kg) and prednisone (Pro) group (i.g. 5 mg/kg) were administrated the drugs for 2 weeks.

Assessment of arthritis severity in mice with collagen-induced arthritis. Arthritis severity was assessed by determining the clinical arthritis grade in all four paws of the mice with a triple blind test. The results were assessed according to a previously described method. Briefly, the severity was scored as follows: 0, normal; 1, mild, apparent swelling limited to individual digits; 2, moderate, redness and swelling of the ankle; 3, redness and swelling in the paw and in the digits; and 4, maximally inflamed leg with the involvement of multiple joints. The arthritis score for each mouse was the sum of arthritis severity scores recorded in all four paws, with 16 points representing the highest score.

Measurement of the spleen index and detection of serum cytokine levels. At the end of the experiment, all mice were sacrificed by cervical dislocation after serum samples were collected. Their spleens were weighed immediately after dissection. The spleen indexes were calculated using the following formula: Spleen Index = Spleen weight / Body weight. The levels of IL-1β and IL-6 in serum samples were measured using commercially available enzyme-linked immunosorbent assay (ELISA) kits according to the standard protocol provided with the kit.

Analysis of histopathology. For the histological analysis of knee joints, the right hind limbs of mice were removed postmortem, fixed with 4% paraformaldehyde for 24 h, decalcified with 12.5% ethylene diamine tetraacetic acid (EDTA, pH 7.0) for 30 days, embedded in paraffin, and then sectioned at a thickness of 6–8 μm. Tissue sections were stained with hematoxylin and eosin prior to observation with a light microscope (Leica, DM2500, Germany). The infiltration of inflammatory cells,

proliferation of synoviocytes, pannus formation, changes in the joint space, cartilage hyperplasia and/or erosion, and bone destruction were blindly graded by a pathologist who assigned scores ranging from 0 to 3 points based on the following criteria: 0, no changes; 1, mild changes; 2, moderate changes; and 3, severe changes.

Imiquimod-induced psoriasis-like skin lesions and scoring of symptoms. Mice were briefly sedated with isoflurane and an area of 5 cm × 4 cm of the back skin of mice was shaved. Two days later, the mice in the control group were administrated a topical treatment with a simple imiquimod base cream (i.e., vehicle), and the mice in the benpyrine groups (i.g. 25, 50 mg/kg) and Pro group (i.g. 5 mg/kg) were administrated the 5% imiquimod cream. Mice were scored daily based on a modified psoriasis area and severity index scoring system, as described previously. Briefly, erythema (redness of the skin) and scaling were scored in a blinded manner on a scale ranging from 0 to 4 points to describe the severity of psoriasis: 0, none; 1, slight; 2, moderate; 3, marked; and 4, very marked. Photos were taken daily to observe the changes in the local skin. At the end-point of the experiment, all mice were euthanized by cervical dislocation. Samples of blood, skin and spleen were collected for future experiments. The skin samples from back lesions were collected in 10% formalin and embedded in paraffin. For the histopathological examination, 3 μm sections were stained with hematoxylin–eosin and observed under a light microscope (Olympus, Tokyo, Japan). Serum were isolated after mice were euthanized. The serum levels of IL-1β and IL-6 in mice were assayed using the ELISA kit as described

above. All procedures were strictly performed according to the manufacturers' instructions.

Statistical methods. Results are presented as means ± standard deviations and were analyzed using SPSS ver. 17.0 software. ANOVA followed by the Student–Newman–Keuls or Wilcoxon rank sum test were utilized for the statistical analyses. $P < 0.05$ was considered a statistically significant difference.

■ AUTHOR INFORMATION

Corresponding Authors

E-mail: zhouyirong@hust.edu.cn (Y. Zhou), zhangyh@mails.tjmu.edu.cn (Y. Zhang), syzyclx@163.com (L. Chen), and li_hua@hust.edu.cn (H. Li).

Authors' Contributions

[#] Weiguang Sun, Yanli Wu and Mengzhu Zheng contributed equally to this work.

Notes

The authors declare no competing financial interest.

■ ACKNOWLEDGMENTS

We acknowledge support from the Program for Changjiang Scholars of Ministry of Education of the People's Republic of China (No. T2016088), the National Science Fund for Distinguished Young Scholars (No. 81725021), the National Natural Science Foundation of China (Nos. 81703580, 81773637, and 81473254) and the

Fundamental Research Fund for the Central Universities (HUST COVID-19 Rapid Response Call, No. 2020kfyXGYJ037, China).

■ ABBREVIATIONS USED

TNF-α, tumor necrosis factor α; RA, rheumatoid arthritis; TNFR, tumor necrosis factor receptor; TACE, TNF-α converting enzyme; ICM, internal coordinate mechanics; MST, microscale thermophoresis; DARTS, drug affinity responsive target stability; NF-κB, nuclear factor kappa-B; LPS, lipopolysaccharide; IκBα, inhibitor of NF-κB α; CIA, collagen-induced arthritis; ELISA, enzyme-linked immunosorbent assay; IL-6, interleukin 6; IPI, imiquimod-induced psoriasiform inflammation

■ ASSOCIATED CONTENT

Supporting Information

The Supporting Information is available free of charge on the ACS Publications website.

Experimental details and spectra for important compounds including NMR spectra HPLC chromatogram as well as computation results (PDF)

■ REFERENCES

1. Wajant, H.; Pfizenmaier, K.; Scheurich, P. Tumor necrosis factor signaling. *Cell Death Differ.* **2003**, *10*, 45–65.

2. Aggarwal, B. B. Signalling pathways of the TNF superfamily: a double-edged sword. *Nat. Rev. Immunol.* **2003**, *3*, 745–756.

3. Lewis; J. D. Anti-TNF antibodies for Crohn's disease--in pursuit of the perfect clinical trial. *N. Engl. J. Med*. **2007**, *357*, 296–298.

4. Palladino, M. A.; Bahjat, F. R.; Theodorakis, E. A.; Moldawer, L. L. Anti-TNF-alpha therapies: the next generation. *Nat. Rev. Drug. Discov.* **2003**, *2*, 736–746.

5. Chaparro, M.; Guerra, I.; Muñoz-Linares, P.; Gisbert, J. P. Systematic review: antibodies and anti-TNF-α levels in inflammatory bowel disease. *Aliment. Pharmacol. Ther.* **2012**, *35*, 971–986.

6. Chen, H. A.; Lin, K. C.; Chen, C. H.; Liao, H. T.; Wang, H. P.; Chang, H. N.; Tsai, C. Y.; Chou, C. T. The effect of etanercept on anti-cyclic citrullinated peptide antibodies and rheumatoid factor in patients with rheumatoid arthritis. *Ann. Rheum. Dis.* **2006**, *65*, 35–39.

7. Vermeire, S.; Noman, M.; Van Assche, G.; Baert, F.; D'Haens, G.; Rutgeerts, P. Effectiveness of concomitant immunosuppressive therapy in suppressing the formation of antibodies to infliximab in Crohn's disease. *Gut.* **2007**, *56*, 1226–1231.

8. Alzani, R.; Corti, A.; Grazioli, L.; Cozzi, E.; Ghezzi, P.; Marcucci, F. Suramin induces deoligomerization of human tumor necrosis factor alpha. *J. Biol. Chem.* **1993**, *268*, 12526–12529.

9. Mancini, F.; Toro, C. M.; Mabilia, M.; Giannangeli, M.; Pinza, M.; Milanese, C. Inhibition of tumor necrosis factor-alpha (TNF-alpha)/TNF-alpha receptor binding by structural analogues of suramin. *Biochem. Pharmacol.* **1999**, *58*, 851–859.

10. He, M. M.; Smith, A. S.; Oslob, J. D.; Flanagan, W. M.; Braisted, A. C.; Whitty, A.; Cancilla, M. T.; Wang, J.; Lugovskoy, A. A.; Yoburn, J. C.; Fung, A. D.; Farrington, G.; Eldredge, J. K.; Day, E. S.; Cruz, L. A.; Cachero, T. G.; Miller, S. K.; Friedman, J. E.; Choong, I. C.; Cunningham, B. C. Small-molecule inhibition of TNF-alpha. *Science* **2005**, *310*, 1022–1025.

11. Sun, H.; Yost, G. S. Metabolic activation of a novel 3-substituted indole-containing TNF-alpha inhibitor: dehydrogenation and inactivation of CYP3A4. *Chem. Res. Toxicol.* **2008**, *21*, 374–385.

12. Deighton, C.; Hyrich, K. International guidelines on access to biologic therapy: why the differences and which is best?. *Nat. Clin. Pract. Rheumatol.* **2008**, *4*, 520–521.

13. Korswagen, L. A.; Bartelds, G. M.; Krieckaert, C. L.; Turkstra, F.; Nurmohamed, M. T.; van Schaardenburg, D.; Wijbrandts, C. A.; Tak, P. P.; Lems, W. F.; Dijkmans, B. A.; van Vugt, R. M.; Wolbink, G. J. Venous and arterial thromboembolic events in adalimumab-treated patients with antiadalimumab antibodies: a case series and cohort study. *Arthritis. Rheum.* **201**, *63*, 877–883.

14. McGeary, R. P.; Bennett, A. J.; Tran, Q. B.; Cosgrove, K. L.; Ross, B. P. Suramin: clinical uses and *structure*-activity relationships. *Mini. Rev. Med. Chem.* **2008**, *8*, 1384–1394.

15. Seidel, S. A.; Dijkman, P. M.; Lea, W. A.; van den Bogaart, G.; Jerabek-Willemsen, M.; Lazic, A.; Joseph, J. S.; Srinivasan, P.; Baaske,

P.; Simeonov, A.; Katritch, I.; Melo, F. A.; Ladbury, J. E.; Schreiber, G.; Watts, A.; Braun, D.; Duhr, S. Microscale thermophoresis quantifies biomolecular interactions under previously challenging conditions. *Methods.* **2013**, *59*, 301–315.

16. Toogood, P. L. Inhibition of protein-protein association by small molecules: approaches and progress. *J. Med. Chem.* **2002**, *45*, 1543–1558.

17. Pai, M. Y.; Lomenick, B.; Hwang, H.; Schiestl, R.; McBride, W.; Loo, J. A.; Huang, J. Drug affinity responsive target stability (DARTS) for small-molecule target identification. *Methods. Mol. Biol.* **2015**, *1263*, 287–298.

18. Martinez, M.D.; Jafari, R.; Ignatushchenko, M.; Seki, T.; Larsson, E.A.; Dan, C.; Sreekumar, L.; Cao, Y.; Nordlund, P. Monitoring drug target engagement in cells and tissues using the cellular thermal shift assay. *Science* **2013**, *341*, 84-87.

19. Chan, D. S.; Lee, H. M.; Yang, F.; Che, C. M.; Wong, C. C.; Abagyan, R.; Leung, C. H.; Ma, D. L. Structure-based discovery of natural-product-like TNF-α inhibitors. *Angew. Chem. Int. Ed.* **2010**, *49*, 2860–2864.

20. Hayden, M. S.; Ghosh, S. Shared principles in NF-kappaB signaling. *Cell* **2008**, *132*, 344–362.

21. Karin, M. Nuclear factor-kappaB in cancer development and progression. *Nature* **2006**, *441*, 431–436.

22. Dong, T.; Li, C.; Wang, X.; Dian, L. Y.; Zhang, X. G.; Li, L.; Chen, S.; Cao, R.; Li, L.; Huang, N.; He, S.; Lei, X. G. Ainsliadimer A selectively inhibits IKKα/β by covalently binding a conserved cysteine. *Nat. Commun.* **2015**, *6*, 6522.

23. Mcinnes, I. B.; Schett, G. Cytokines in the pathogenesis of rheumatoid arthritis. *Nat. Rev. Immunol.* **2007**, *7*, 429–442.

24. Simsek, I. TNF inhibitors - new and old agents for rheumatoid arthritis. *Bulletin of the NYU Hospital for Joint Diseases.* **2010**, *68*, 204–210.

25. Okroj, M.; Heinegård, D.; Holmdahl, R.; Blom, A. M. Rheumatoid arthritis and the complement system. *Ann. Med.* **2007**, *39*, 517–530.

26. Vincent, F. B.; Morand, E. F.; Murphy, K.; Mackay, F.; Mariette, X.; Marcelli, C. Antidrug antibodies (ADAb) to tumour necrosis factor (TNF)-specific neutralising agents in chronic inflammatory diseases: a real issue, a clinical perspective. *Ann. Rheum. Dis.* **2013**, *72*, 165–178.

27. Perera, G. K.; Di Meglio, P.; Nestle, F. O. Psoriasis. *Annu. Rev. Pathol.* **2012**, *7*, 385-422.

28. Elder, J. T.; Bruce, A. T.; Gudjonsson, J. E.; Johnston, A.; Stuart, P. E.; Tejasvi, T.; Voorhees, J. J.; Abecasis, G. R.; Nair, R. P. Molecular dissection of psoriasis: integrating genetics and biology. *J. Invest. Dermatol.* **2010**, *130*, 1213–1226.

29. Leonardi, C. L.; Powers, J. L.; Matheson, R. T.; Goffe, B. S.; Zitnik, R.; Wang, A.; Gottlieb, A. B.; Etanercept Psoriasis Study Group. Etanercept as monotherapy in patients with psoriasis. *N. Engl. J. Med.* **2003**, *349*, 2014–2022.

30. Strand, V.; Balsa, A.; Al-Saleh, J.; Barile-Fabris, L.; Horiuchi, T.; Takeuchi, T.; Lula, S.; Hawes, C.; Kola, B.; Marshall, L. Immunogenicity of Biologics in Chronic Inflammatory Diseases: A Systematic Review. *Biodrugs* **2017**, *31*, 299–316.

31. Swindell, W. R.; Johnston, A.; Carbajal, S.; Han, G.; Wohn, C.; Lu, J.; Xing, X.; Nair, R. P.; Voorhees, J. J.; Elder, J. T.; Wang, X. J.; Sano, S.; Prens, E. P.; DiGiovanni, J.; Pittelkow, M. R.; Ward, N. L.; Gudjonsson, J. E. Genome-wide expression profiling of five mouse models identifies similarities and differences with human psoriasis. *Plos One* **2011**, *6*, e18266.

32. Lundkvist, J.; Kastäng, F.; Kobelt, G. The burden of rheumatoid arthritis and access to *treatment*: health burden and costs. *Eur. J. Health. Econ.* **2008**, *8*, S49–S60.

33. Varfolomeev, E. E.; Ashkenazi, A. Tumor necrosis factor: an apoptosis JuNKie?. *Cell* **2004**, *116*, 491–497.

34. Wang, L.; Du, F.; Wang, X. TNF-alpha induces two distinct caspase-8 activation pathways. *Cell* **2008**, *133*, 693–703.

35. Rubbert-Roth, A.; Finckh, A. Treatment options in patients with rheumatoid arthritis failing initial TNF inhibitor therapy: a critical review. *Arthritis res. Ther.* **2009**, *11*, Suppl 1, S1.

36. Esposito, E.; Cuzzocrea, S. TNF-alpha as a therapeutic target in inflammatory diseases, ischemia-reperfusion injury and trauma. *Curr. Med. Chem.* **2009**, *16*, 3152–3167.

37. Bourne, T.; Fossati, G.; Nesbitt, A. A. PEGylated Fab' fragment against tumor necrosis factor for the treatment of Crohn disease: exploring a new mechanism of action. *Biodrugs* **2008**, *22*, 331–337.

38. Goldbach-Mansky, R.; Lipsky, P. E. New concepts in the treatment of rheumatoid arthritis. *Annu. Rev. Med.* **2003**, *54*, 197–216.

39. Hasegawa, A.; Takasaki, W.; Greene, M. I.; Murali, R. Modifying TNF alpha for therapeutic use: a perspective on the TNF receptor system. *Mini. Rev. Med. Chem.* **2001**, *1*, 5–16.

40. Neves, M. A.; Totrov, M.; Abagyan, R. Docking and scoring with ICM: the benchmarking results and strategies for improvement. *J. Comput. Aided. Mol. Des.* **2012**, *26*, 675–686.

41. Litchfield, J. T.; Wilcoxon, F. A simplified method of evaluating dose-effect experiments. *J. Pharmacol. Exp. Ther.* **1949**, *96*, 99–113.

Legends of Figures

Figure 1. Benpyrine is a novel and potent TNF-α inhibitor. (A) Chemical structures of benpyrine and SPD304. (B) Inhibition of TNF-α-induced cell death. The inhibitory effect was measured at different concentrations (1 and 10 μM). Survival rates are reported as averages ± SD. Each experiment was repeated three times. (C) Morphology of L929 cells after treatment with actinomycin D, actinomycin D with TNF-α, and pretreatment with 1 or 10 μM benpyrine and 10 μM SPD304.

Figure 2. Benpyrine inhibits the binding of TNF-α to TNFR1. (A-D) The interactions of benpyrine (A) or TNFR1 (B) with TNF-α were quantified using the MST method. After an incubation with 10 (C) or 100 (D) μM benpyrine, the K_D values of TNF-α with TNFR1 were significantly increased. (E) Benpyrine inhibited TNFR1 binding to immobilized TNF-α. (F) Benpyrine protected the target protein TNF-α from proteases. (G) Benpyrine protected the target protein TNF-α from high temperatures. (H) Binding pose of benpyrine binding in the allosteric site of TNF-α, The TNF-α model was generated based on the co-crystal structure of TNF-α with SPD304 (PDB ID: 2AZ5) and was portrayed as a cartoon. (I) Diagram showing the interaction of the benpyrine ligand with TNF-α.

Figure 3. Benpyrine directly binds TNF-α and blocks the downstream NF-κB-mediated inflammatory signaling. (A) The cytotoxicity of wild type and mutant TNF-α proteins toward L929 cells. (B) The protective effects of benpyrine on the inflammation caused by different TNF-α proteins. (C) The binding of benpyrine to different TNF-α proteins detected using the MST assay. (D-E) RAW264.7 cells were preincubated with the indicated concentrations of benpyrine for 12 h prior to stimulation with 10 ng/mL TNF- α or 1 μg/mL LPS. The cells were harvested after 2 h, and the total cell lysates were examined for the occurrence of IκBα phosphorylation using western blot experiments. (F) NF-κB activation was detected by assessing its nuclear translocation. RAW264.7 cells were treated with 10 ng/mL TNF-α in the absence or presence of benpyrine for 2 h. Then, NF-κB/p65 nuclear translocation was

investigated by staining cells with an anti-p65 subunit antibody (red) and DAPI (blue).

Figure 4. The protective effects of benpyrine on mice with LPS-induced endotoxemia. (A-B) Serum IL-6 and IL-1β levels were examined at 24 h after the LPS (1.5 mg/kg, i.p) injections in mice using ELISAs. (C) The effects of benpyrine on the survival rate in mice with endotoxemia induced by LPS. (D) Images of H&E staining in liver and lung sections from control, LPS (15 mg/kg, i.p) and benpyrine-treated mice. Less sinusoidal cell loss, tissue destruction and hemorrhaging were observed after the benpyrine treatments. Data are presented as means ± SD; $^{\#\#}$ $P < 0.01$ compared with samples from the normal group; * $P < 0.05$ and ** $P < 0.01$ compared with the LPS group (n = 10 mice per group).

Figure 5. Therapeutic effect of benpyrine on CIA mice. (A) Arthritis scores were recorded for 7 weeks after the first collagen injection. Mice treated with benpyrine exhibited a remarkable amelioration of the arthritis score. (B) Benpyrine decreased the spleen index of CIA mice. (C-F) Effects of benpyrine on the serum levels of IFN-γ, IL-6, IL-1β, IL-17 and IL-10. (G) Effects of benpyrine on the histopathological changes in the ankle joints of CIA mice. CIA mice treated with benpyrine (25, 50 mg/kg) and prednisone (5 mg/kg) showed less inflammatory cell infiltration, well preserved joint spaces and minimal synovial hyperplasia. Data are presented as means ± SD; $^{\#\#}$ $P < 0.01$ compared with samples from the normal group; * $P < 0.05$ and ** $P < 0.01$ compared with the CIA group (n = 10 mice per group).

Figure 6. The therapeutic effects of benpyrine on imiquimod-induced psoriasiform inflammation in mice. (A) Representative images of imiquimod-induced psoriasis-like lesions in mice treated with imiquimod or the control cream for 6 consecutive days. (B) Clinical scores for scaling were assessed to monitor disease severity. (C-E) The spleen index and relative levels of IL-1β and IL-6 in serum were measured using ELISAs. (F) Representative images of H&E-stained back skin sections on day 7, magnification 200 ×. Data are presented as means ± SD; $^{\#}$ $P < 0.05$ and $^{\#\#}$ $P < 0.01$ compared with samples from the normal group; * $P < 0.05$ and ** $P < 0.01$ compared with the CIA group (n = 10 mice per group).

Figure 1. Benpyrine is a novel and potent TNF-α inhibitor.

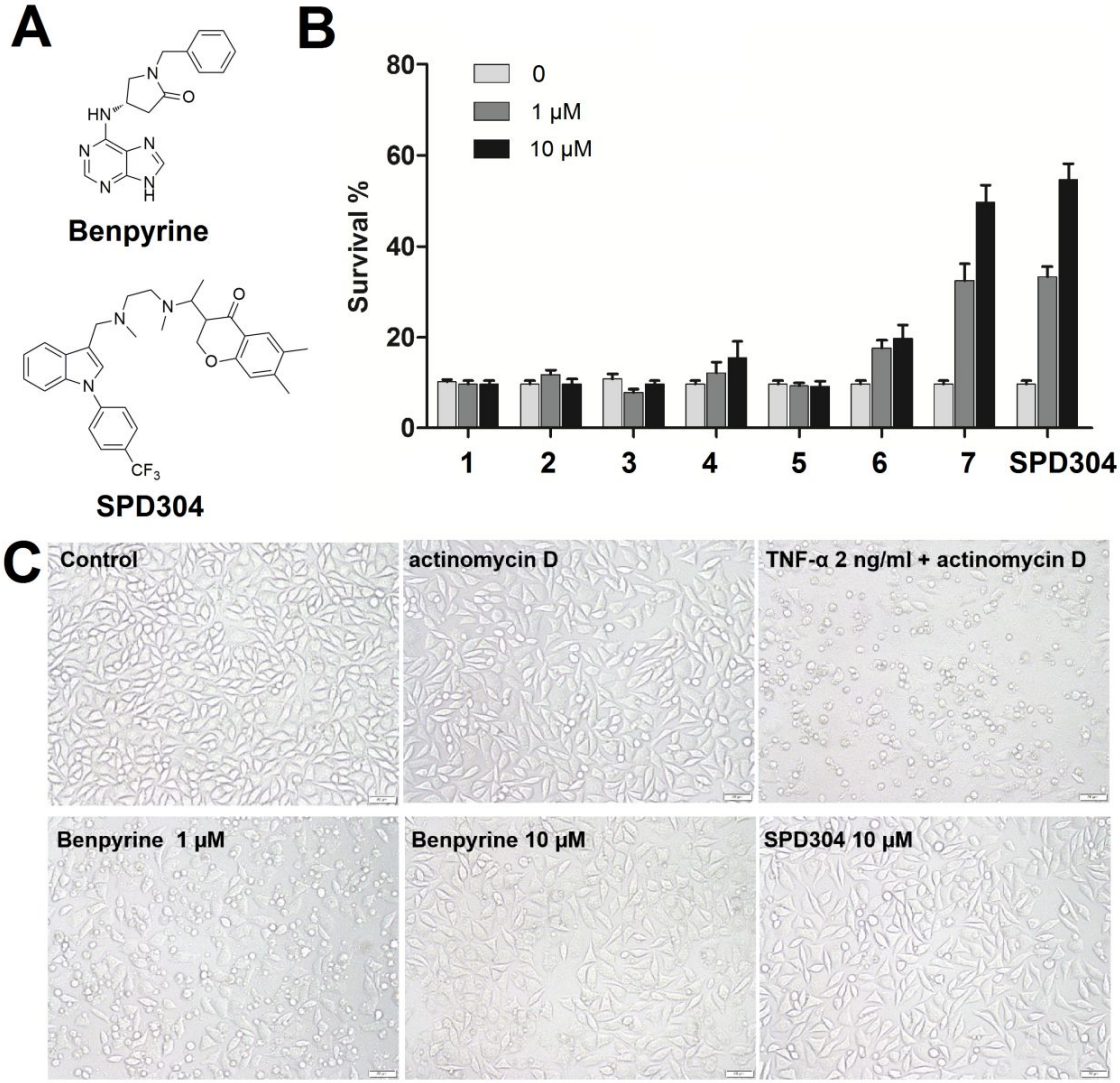

Figure 2. Benpyrine inhibits the binding of TNF-α to TNFR1.

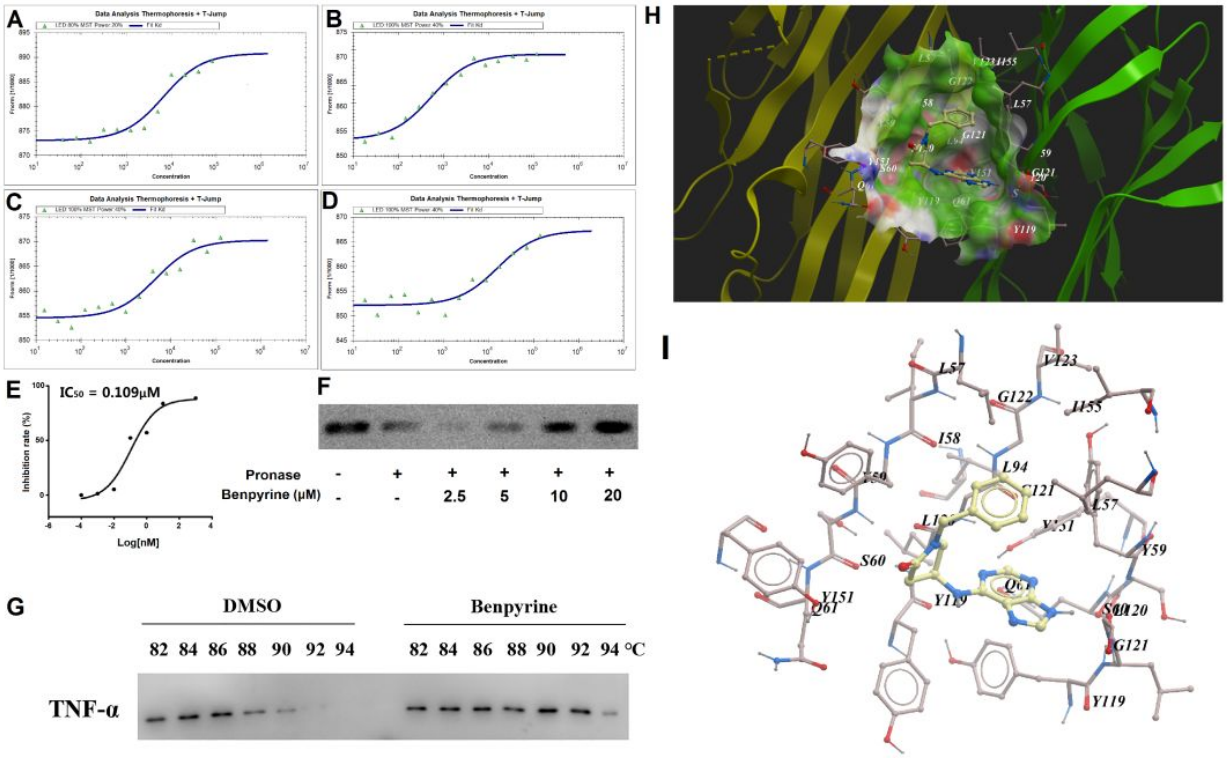

Figure 3. Benpyrine directly binds TNF-α and blocks the downstream NF-κB-mediated inflammatory signaling.

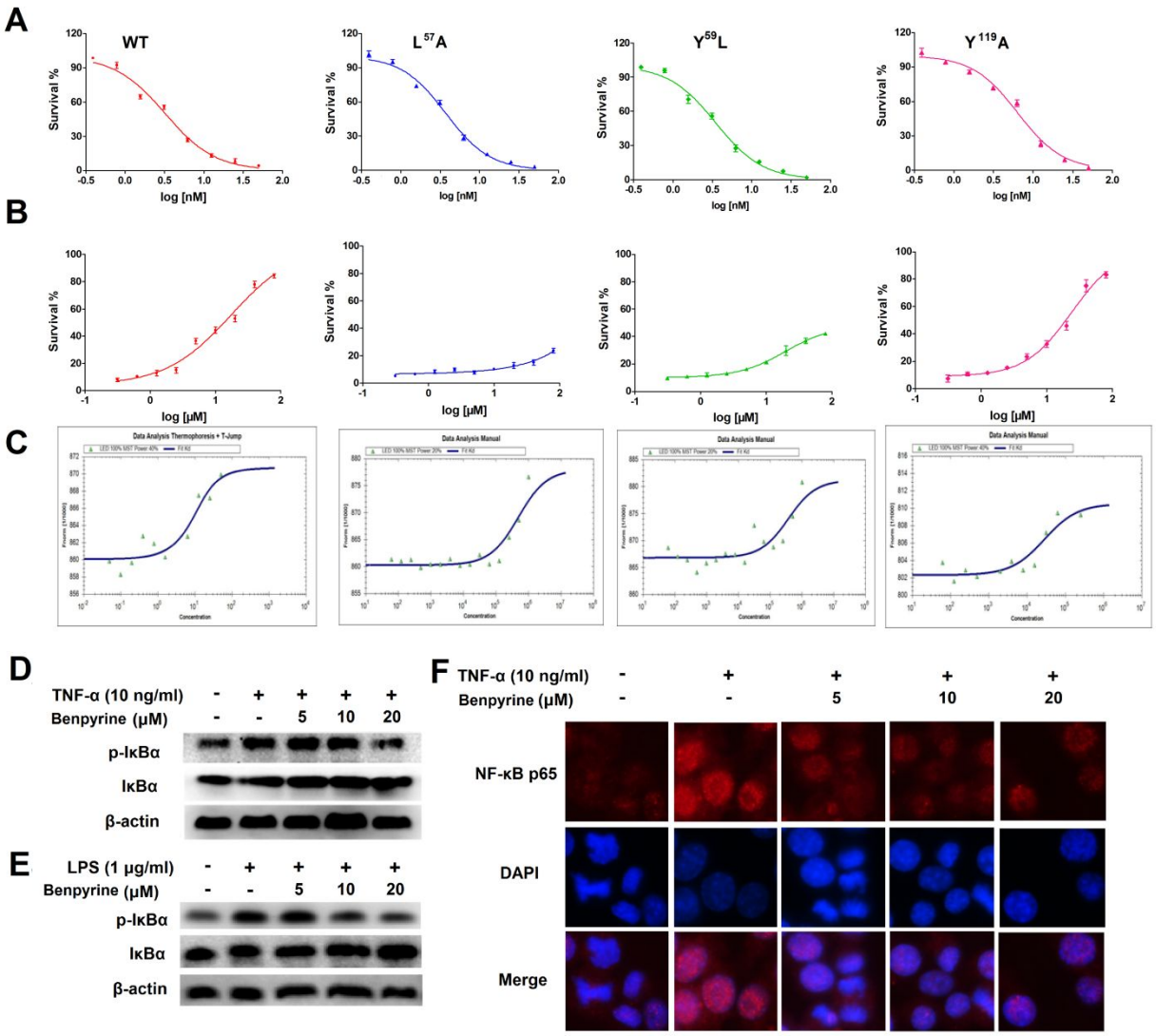
A
WT
L57A
Y59L
Y119A
Survival %
log [nM]
B
Survival %
log [μM]
C
Data Analysis Thermophoresis + T-Jump
Data Analysis Manual
D
TNF-α (10 ng/ml) - + + + +
Benpyrine (μM) - - 5 10 20
p-IκBα
IκBα
β-actin
E
LPS (1 μg/ml) - + + + +
Benpyrine (μM) - - 5 10 20
p-IκBα
IκBα
β-actin
F
TNF-α (10 ng/ml) - + + + +
Benpyrine (μM) - - 5 10 20
NF-κB p65
DAPI
Merge

Figure 4. The protective effects of benpyrine on mice with LPS-induced endotoxemia.

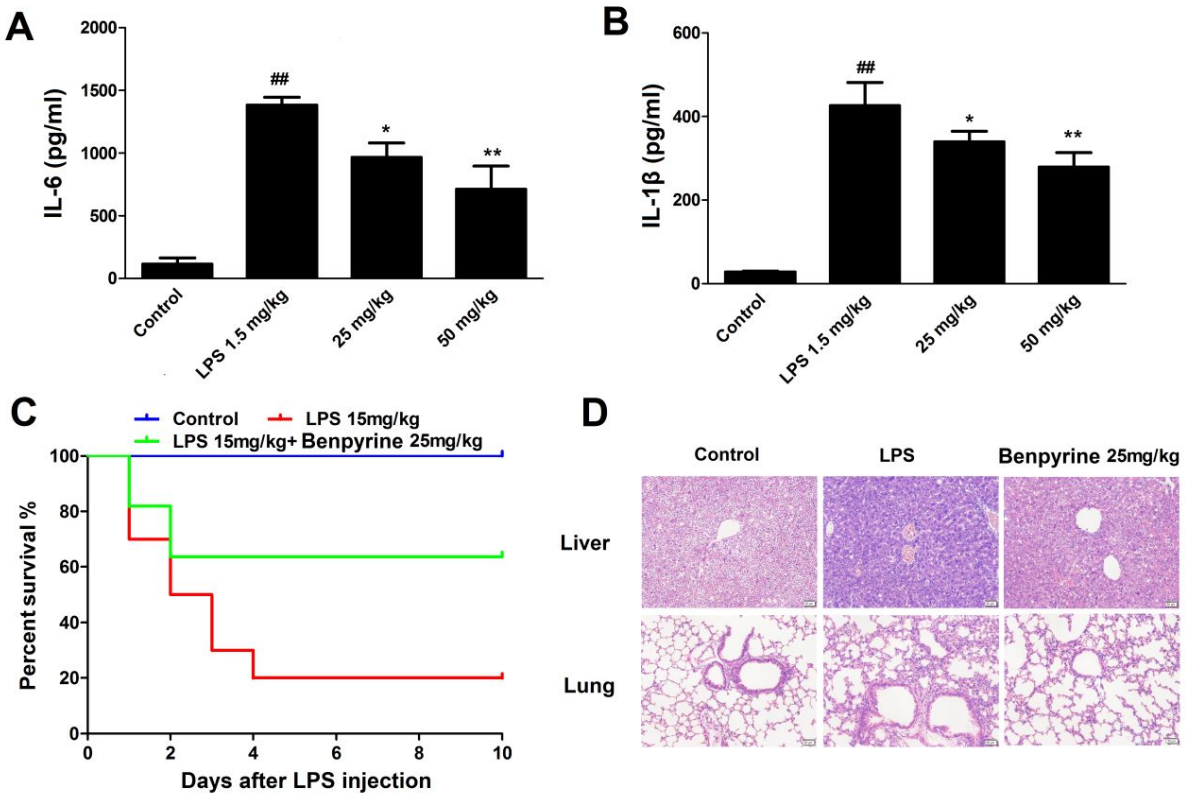

Figure 5. Therapeutic effect of benpyrine on CIA mice.

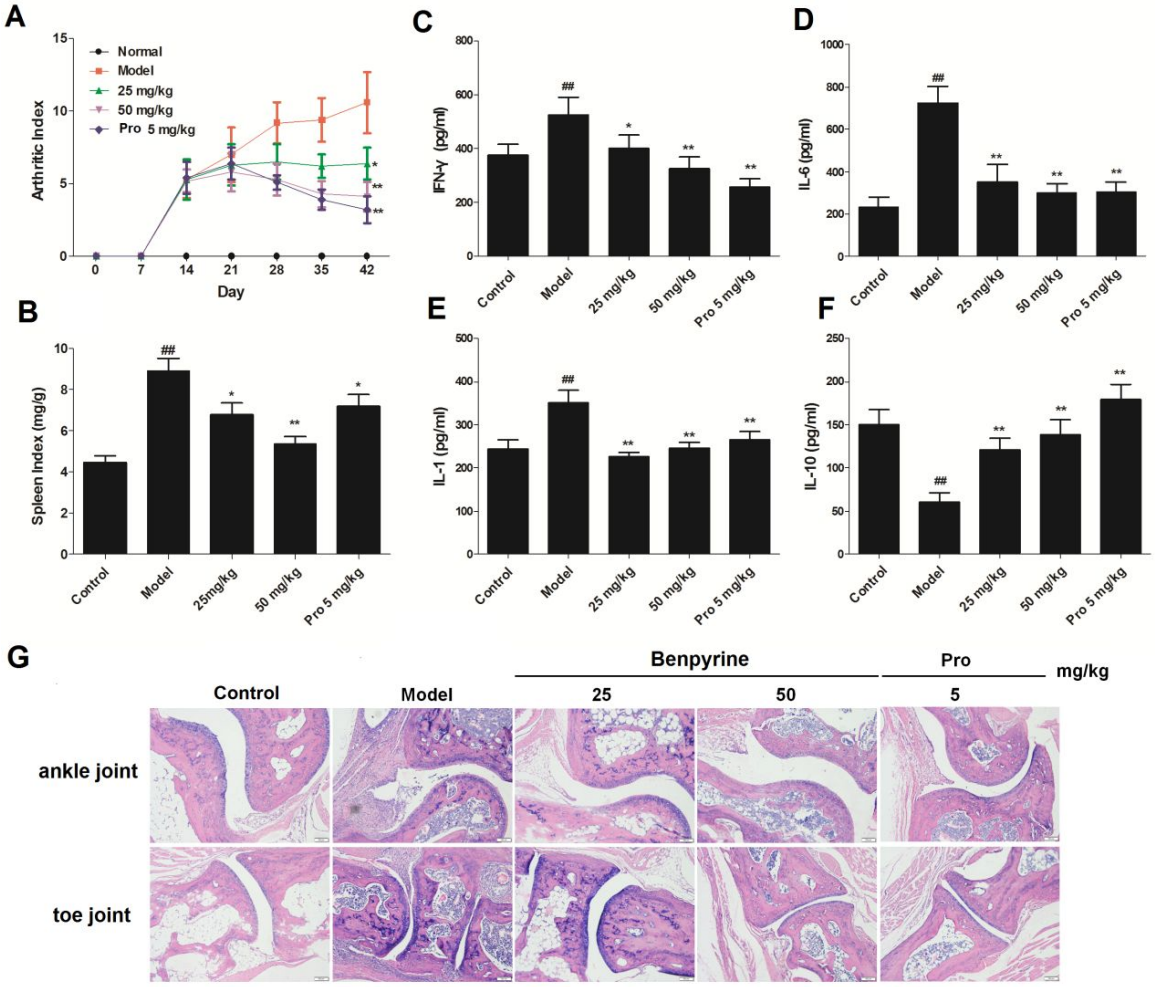

Figure 6. The therapeutic effects of benpyrine on imiquimod-induced psoriasiform inflammation in mice.

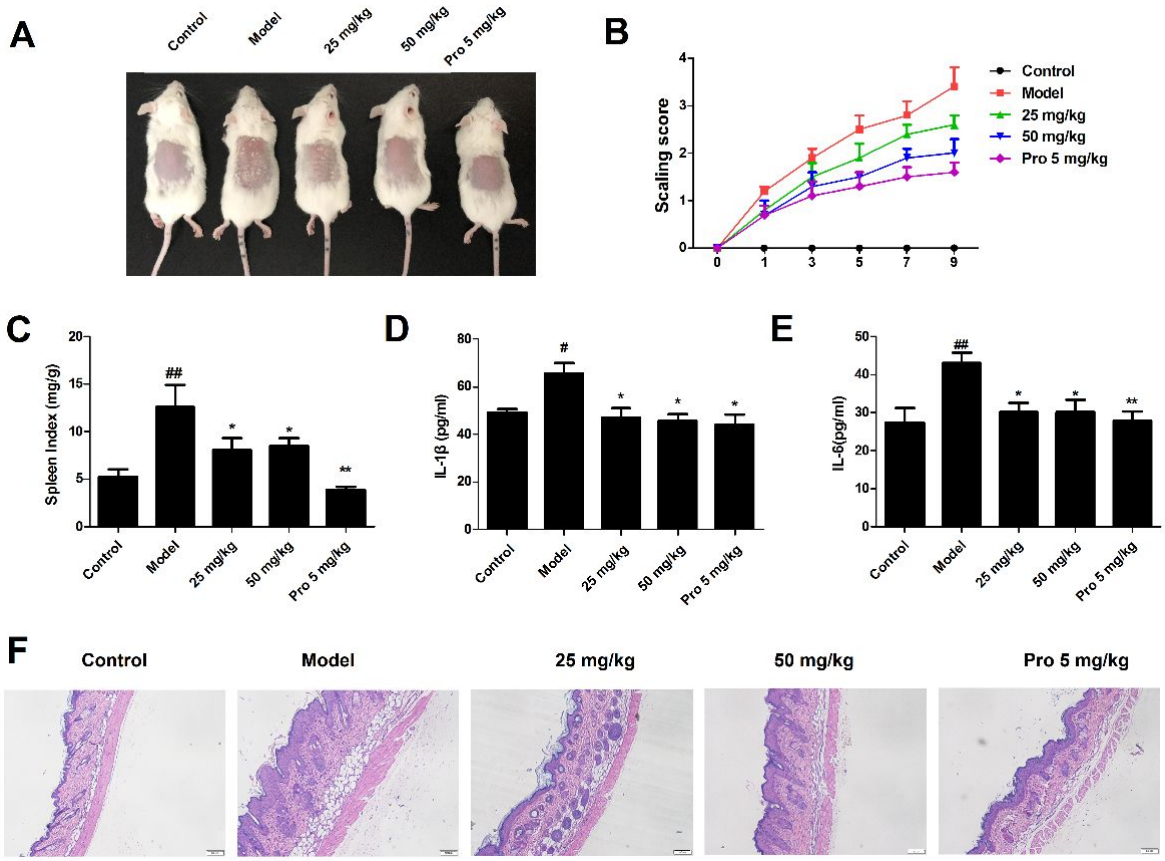

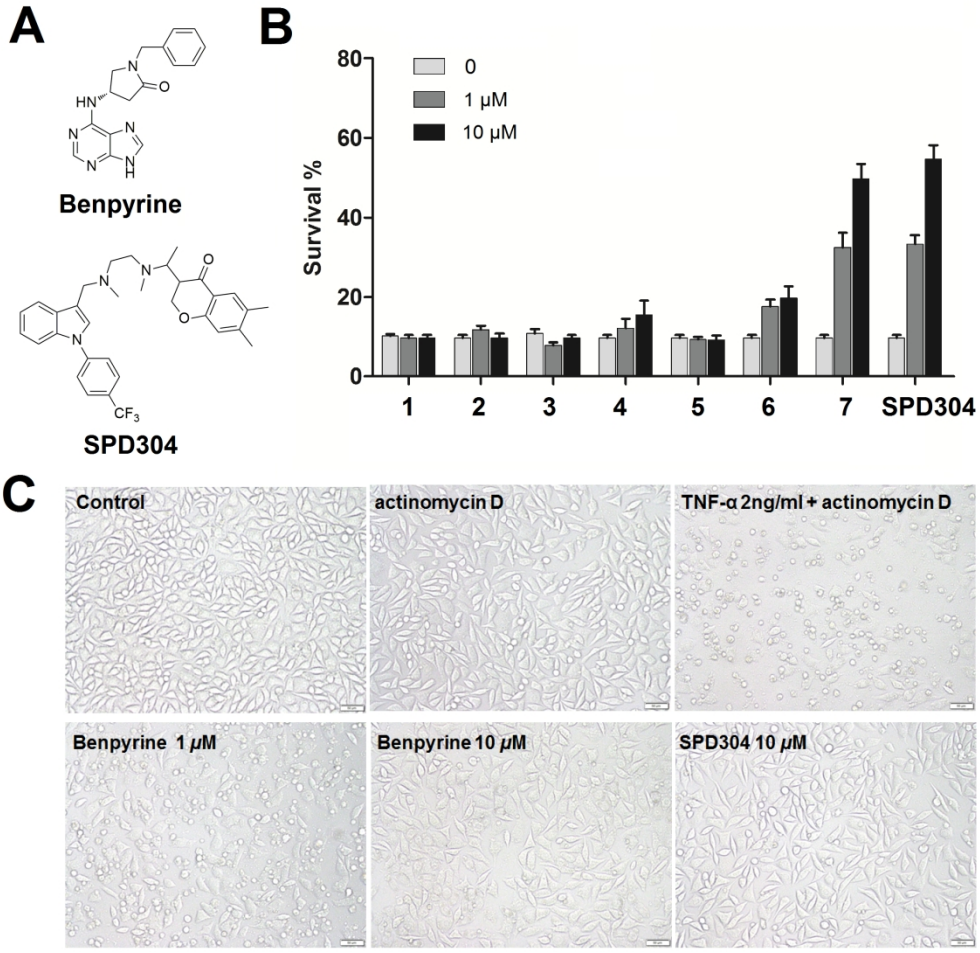

Figure 1. Benpyrine is a novel and potent TNF-α inhibitor. (A) Chemical structure of benpyrine and SPD304. (B) Inhibition of TNF-α induced cell. The inhibition was measured in different concentrations (1 and 10 μM). Survive rates were determined as average ± SD. Each experiment has been repeated three times. (C) Morphology of L929 cells after treated with actinomycin D, actinomycin D with TNF-α, pretreatment with 1 or 10 μM benpyrine and 10 μM SPD304.

499x477mm (144 x 144 DPI)

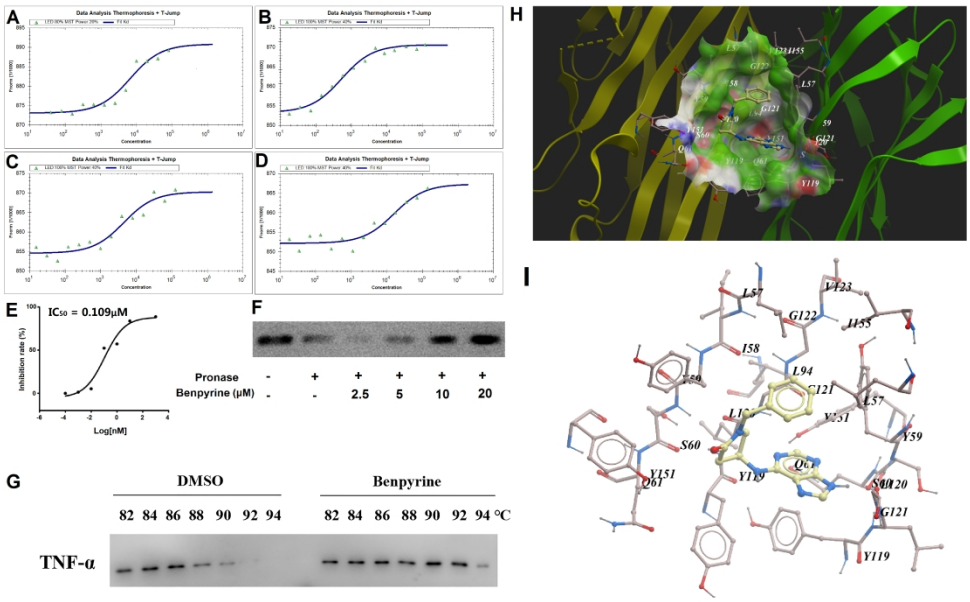

Figure 2. Benpyrine inhibits the binding of TNF-α to TNFR1. (A-D) The interactions of benpyrine (A) or TNFR1 (B) with TNF-α were quantified using the MST method. After an incubation with 10 (C) or 100 (D) μM benpyrine, the KD values of TNF-α with TNFR1 were significantly increased. (E) Benpyrine inhibited TNFR1 binding to immobilized TNF-α. (F) Benpyrine protected the target protein TNF-α from proteases. (G) Benpyrine protected the target protein TNF-α from high temperatures. (H) Binding pose of benpyrine binding in the allosteric site of TNF-α, The TNF-α model was generated based on the co-crystal structure of TNF-α with SPD304 (PDB ID: 2AZ5) and was portrayed as a cartoon. (I) Diagram showing the interaction of the benpyrine ligand with TNF-α.

398x254mm (360 x 360 DPI)

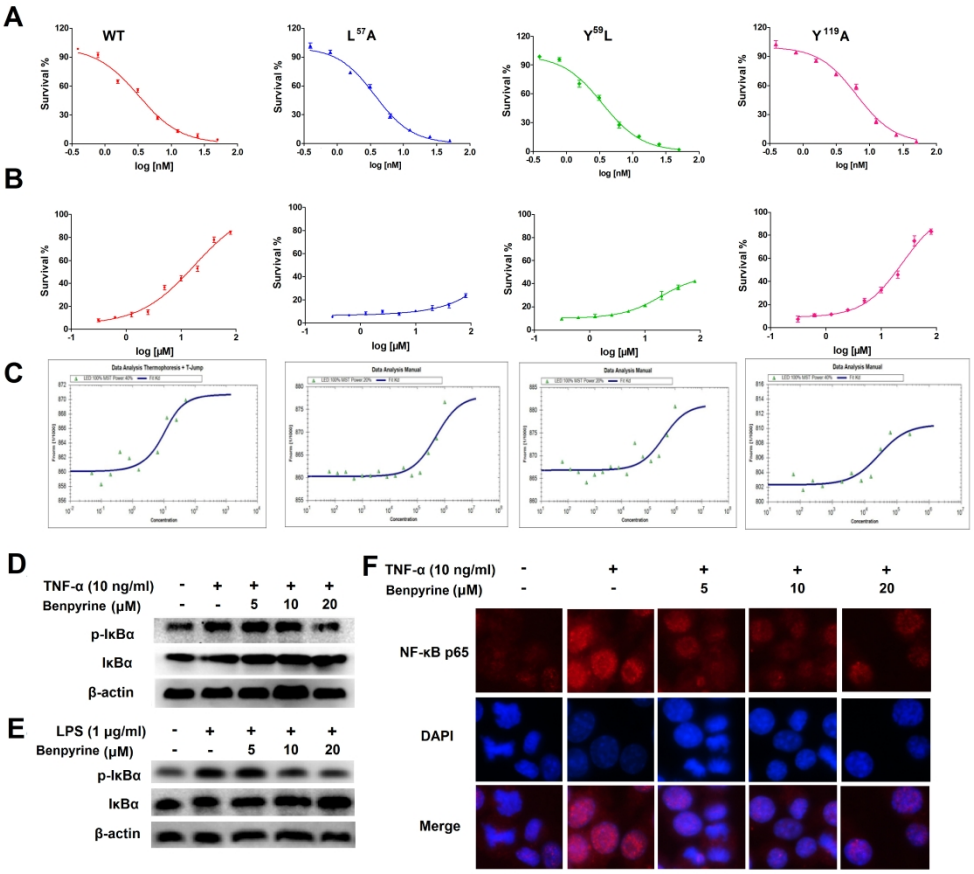

Figure 3. Benpyrine directly binded with TNF-α and blocked the downstream NF-κB inflammation signal. (A) The cytotoxicity of wide type and mutant TNF-α proteins on L929 cells. (B) The protection effects of benpyrine against different type of TNF-α proteins. (C) The binging abilities of benpyrine with different type of TNF-α proteins detected with MST. (D-E) RAW264.7 cells were preincubated with the indicated concentrations of benpyrine for 12 h before stimulation with 10 ng/mL TNF- α or 1 μg/mL LPS. The cells were harvested after 2 h, and the total cell lysates were tested via Western blot experiments for the occurrence of IκBα phosphorylation. (F) NF-κB activation detected by nuclear translocation. RAW264.7 cells were treated with 10 ng/mL TNF- α in the absence or presence of benpyrine for 2 h. Then, NF-κB/p65 nuclear translocation was investigated by staining with an anti-p65 subunit antibody (red) and DAPI (blue).

904x808mm (144 x 144 DPI)

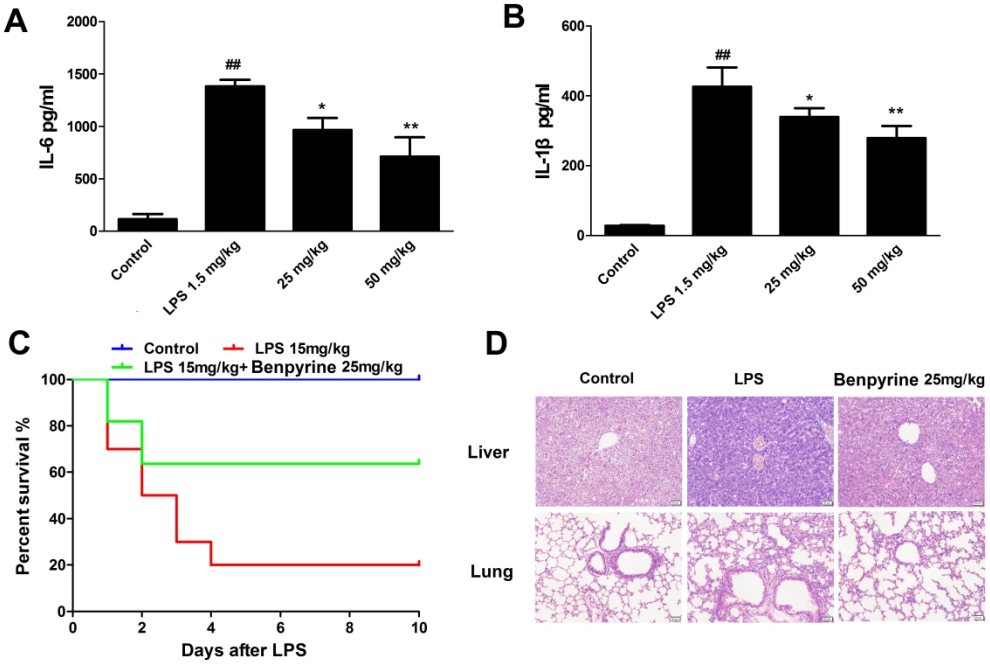

Figure 4. The protective effects of benpyrine in LPS induced endotoxemic mice. (A-B) Serum IL-6 and IL-1β levels were examined at 24 h though ELISA after LPS (1.5 mg/kg, i.p) induced in mice. (C) The effects of benpyrine on endotoxemia survival rate in mice induced by LPS (15 mg/kg, i.p). (D) H&E staining of sections from liver and lung in control, LPS (15 mg/kg, i.p) and benpyrine treated mice. Less sinusoidal cells loss, tissue destruction and hemorrhage were observed after benpyrine treatments. Data are expressed as means ± SD; ## $P < 0.01$ compared with sample of normal group, * $P < 0.05$, ** $P < 0.01$ compared with the LPS group (n = 10 in each group).

962x654mm (144 x 144 DPI)

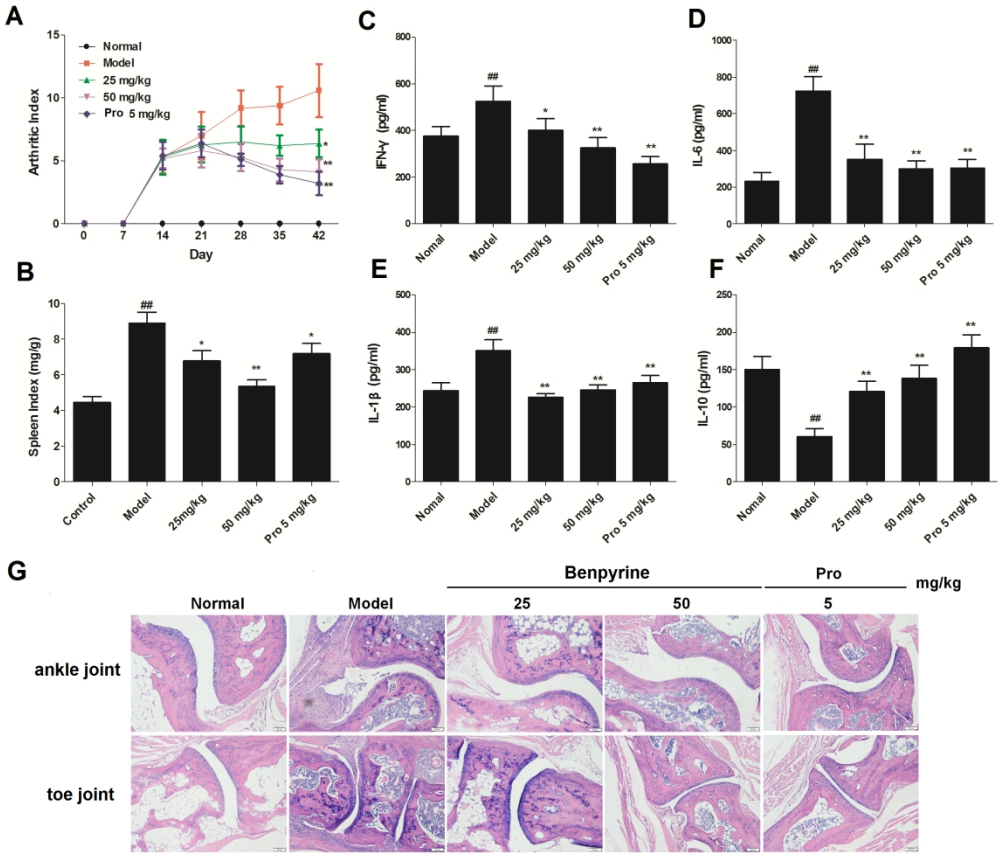

Figure 5. Therapeutic effect of benpyrine on CIA mice. (A) Arthritis scores were recorded for 7 weeks after the first collagen injection. Mice treated with benpyrine exhibited a remarkable amelioration of the arthritis score. (B) Benpyrine decreased the spleen index of CIA mice. (C-F) Effects of benpyrine on the serum levels of IFN-γ, IL-6, IL-1β, IL-17 and IL-10. (G) Effects of benpyrine on the histopathological changes in the ankle joints of CIA mice. CIA mice treated with benpyrine (25, 50 mg/kg) and prednisone (5 mg/kg) showed less inflammatory cell infiltration, well preserved joint spaces and minimal synovial hyperplasia. Data are presented as means ± SD; ## $P < 0.01$ compared with samples from the normal group; * $P < 0.05$ and ** $P < 0.01$ compared with the CIA group (n = 10 mice per group).

484x416mm (144 x 144 DPI)

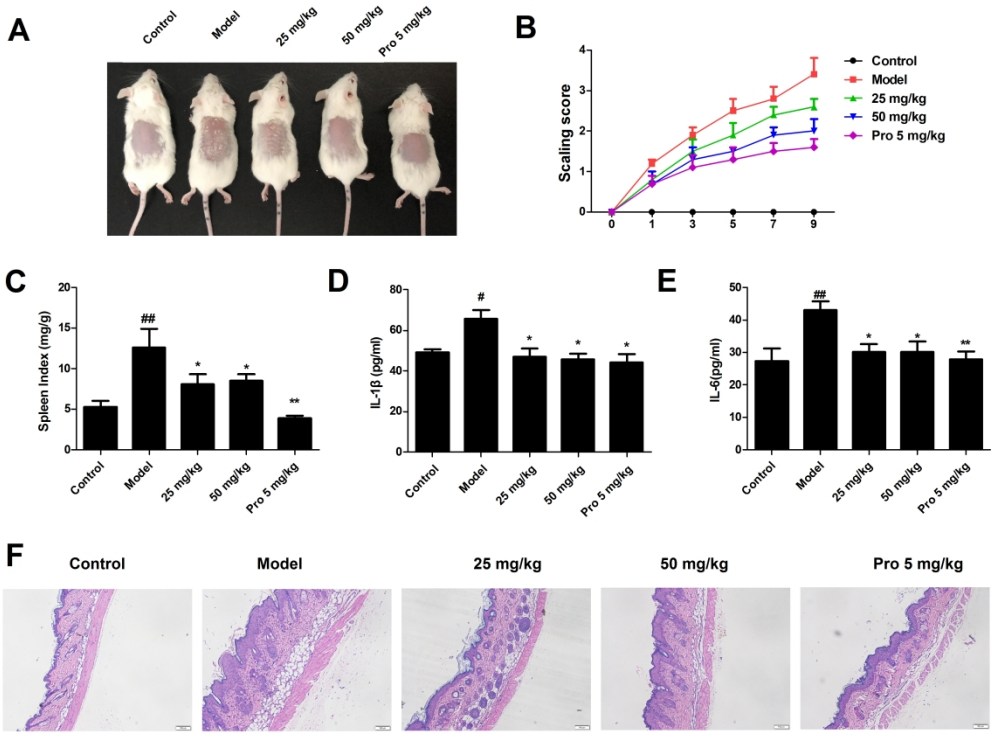

Figure 6. The therapy effects of benpyrine on imiquimod-induced psoriasiform inflammation mice. (A) Representative image of imiquimod-induced psoriasis-like lesions in mice treated with imiquimod or control cream for 6 consecutive days. (B) Clinical scores for scaling score were assessed for disease severity. (C-E) Spleen index and relative expression of IL-1β and IL-6 in serum were measured by Elisa method. (F) Representative H&E-stained back skin sections on day 7, magnification 200 ×. Data are expressed as means ± SD; # $P < 0.05$, ## $P < 0.01$ compared with sample of normal group, * $P < 0.05$, ** $P < 0.01$ compared with the CIA group (n = 10 in each group).

805x597mm (144 x 144 DPI)

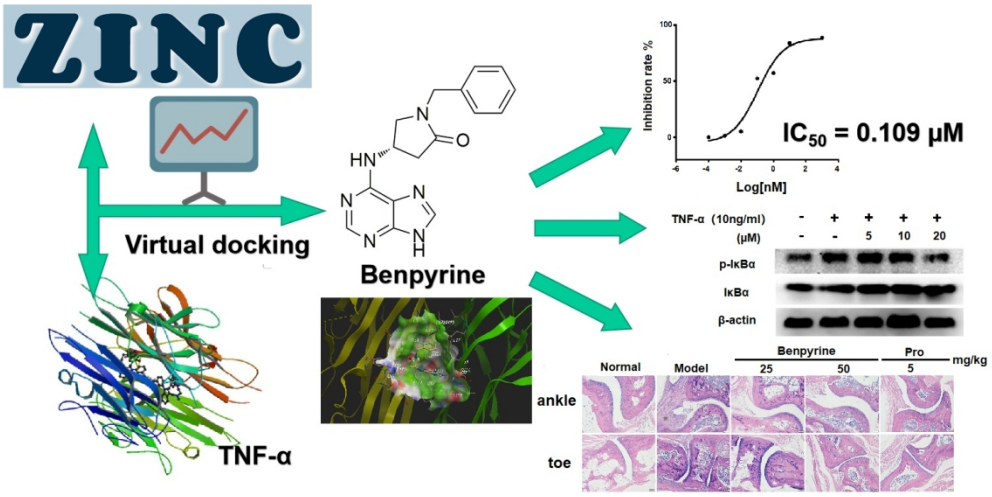
ZINC
Virtual docking
Benpyrine
TNF-α
Inhibition rate %
Log[nM]
IC50 = 0.109 μM
TNF-α (10ng/ml)
(μM)
p-IκBα
IκBα
β-actin
Normal
Model
Benpyrine
Pro
mg/kg
ankle
toe